

# Detailed Observations of Convective Instability on an Interfacial Salty Layer

R. Abdeljabar<sup>1</sup>, F. Onofri<sup>2</sup> and M.J. Safi<sup>1</sup>

**Abstract:** This paper focuses on the mechanisms of convective instability in a stable salty gradient layer (i.e. an interfacial salty layer). This layer is assumed to be initially confined between two homogeneous liquid layers: a lower layer composed of salty water of 5wt% concentration and an upper layer composed of distilled water. The mechanisms underlying the interfacial salty layer's instability are depicted experimentally using a PIV technique and via measurements of concentration and temperature. It is found that in addition to the effect of double-diffusion across the interfacial salty layer, different forms of Kelvin-Helmholtz instability occur at different locations:

- i. At the edge of the interfacial salty layer adjacent to the upper layer;
- ii. At the edge of the interfacial salty layer adjacent to the lower layer;
- iii. Within the interfacial salty layer itself.

The first induces horizontal moving of the interfacial layer liquid that is initially at rest. The second acts by sweeping the lower edge of the interfacial layer due to convective flows. In particular, the kinetic energy of the convective flows at the lower edge of the interfacial layer combine with the effect of double diffusion (i.e. the salty gradient layer become weaker) to generate a patch of overturning flows. This phenomenon induces the mixing of the stable interfacial layer by overturning flows that gradually erode the layer. The third effect acts by tearing the interfacial layer under the action exerted by convective vortices at the adjacent boundaries.

**Keyword:** Convective shear flows, double-diffusion, erosion, instability.

## 1 Introduction

The problem of stability in a double-diffusive thermohaline system has received considerable attention, most of which consists of analytical and experimental studies on the stability of salty gradient layers [e.g. Barenblatt et al. (1993); Baines and Gill (1963); Bars and Davaille (2002); Bergman et al. (1987); Huppert (1971); Harindra (1987); Turner (1968); Veronis (1968); Walton (1982); Wright and Loehr (1976); Zangrando and Bertran (1985)]. Although, some well-established theories are available [e.g. Baines and Mitsudera (1994); Chandrasekhar (1961); Drazin (1981)], the physics of the mechanisms that cause instability by shear convective flows requires additional investigation. This is in contrast to case of turbulent instability where the physical causes have been identified, see for instance [Balmforth et al. (1998); Galimiche and Hunt (2002)].

Numerous mechanisms, which lead to instability in thermosolutal systems, have been studied. The double-diffusion transport phenomenon across interfaces is one of them. Several experimental and theoretical studies of double-diffusion in salty stratified layers have been performed [e.g. Linden and Shirtcliffe (1978); Turner (1973)]. The entrainment and mixing of a salty gradient layer heated from below has also been studied [e.g. Hull and Mehta (1987); Khantha et al. (1977); Linden (1975); Park et al. (1994); Poplowsky et al. (1981); Turner (1991); Wyatt (1978)]. The study of the turbulent entrainment of interfacial layers in stratified fluids has been restricted mainly to the determination of an average entrainment rate expressed in terms of overall length, velocity and density scales of the flow usually expressed in terms of a Richardson number ( $R_i$ ). A flux Richardson number has also been used, which depends on an overall Richardson number

<sup>1</sup> URME, National School of Engineers of Tunis, B.P 37, 1002 Belvedere, Tunisia

<sup>2</sup> Ecole Polytechnique de mécanique énergétique, CNRS, Marseille cedex, France

and a Peclet number ( $R_f = \frac{u_e}{U} = f(R_{io}, P_e)$ ) or by a series of power laws over limited range of  $R_i$  [e.g. Linden and Shirtcliffe (1978); Harindra et al. (1985); Sulliva and John (1994)].

Most of the experiments in the previous studies have been performed under a constant heat-flux boundary condition. Similarly, other experiments under constant temperature heating have been performed [Abdeljabar and Safi (2000)] in which, similarly to the constant flux heating cases, the same evolution of the stratification has been observed. Recently, some experimental studies [Abdeljabar and Safi (2001)] revealed that the interfacial layer is sheared by vortices located near the edges of the interfacial layer.

The interfacial layer between two homogeneous liquid layers, which are flowing relative to each other, is unstable, and the resulting growing wave is well known as Kelvin-Helmholtz instability [e.g. Chandrasekhar (1961)]. This Kelvin-Helmholtz instability occurs when a critical Richardson number ( $R_i = N^2 / (\frac{\partial u}{\partial z})^2$  where  $N^2 = -\frac{g}{\rho_m} (\frac{\partial \rho}{\partial z})$ :  $N$  is Brunt frequency, and  $(\frac{\partial u}{\partial z})$  gradient of velocity) is reached [see. Chandrasekhar (1961) or Drazin (1989)]. The critical Richardson number for which instability occurs is equal to  $R_i = 1/4$ ; i.e. the Miles-Howard criterion. Unfortunately, this criterion does not provide sufficient insights into the mechanics of the instability process. Thus, the study of shear flows in thermohaline systems can shed light on generative mechanisms of instability that have not yet been fully understood.

The present paper reports the mechanisms of instability within the interfacial layer (i.e. salty gradient layer between two homogeneous layers) due to convective flows. A 2D-PIV technique was utilized throughout the stratification. The focus of the present study is on the interfacial layer evolution. Moreover, temperature and concentration variations were measured in the adjacent homogeneous layers. Also, the velocity profiles of the interfacial layer were investigated. The basic idea behind PIV measurements is to visualize the instability due to shear convective flows. All of these measurements lead us to explain the mechanisms, which enhance the instability of the inter-

facial layer and cause it's mixing into the adjacent homogeneous layers.

## 2 Experimental Study

### 2.1 Experimental Apparatus

The experiment was performed in a rectangular Plexiglas tank with inner dimension of 100mm×40mm×50mm. The Plexiglas wall is 20mm thick. The bottom of the tank is a copper plate of 10mm thickness from which heat was supplied at constant temperature. Figure 1 presents a synopsis of the experimental apparatus. More details on the experimental apparatus can be found in [Abdeljabar and Onofri (2004)].

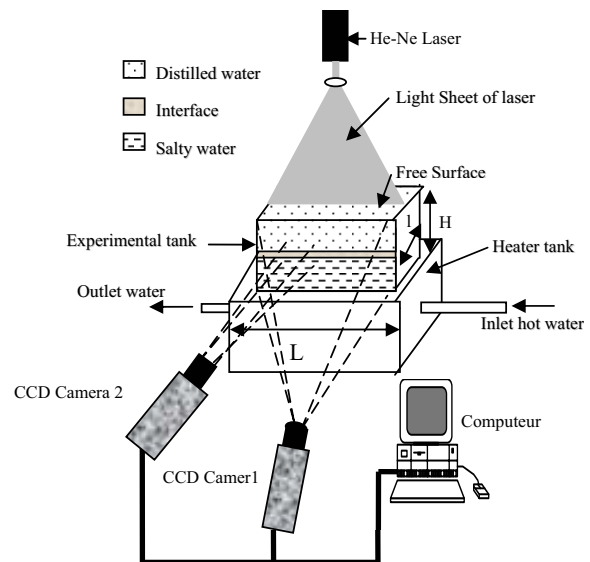


Figure 1: Sketch of the Experimental device

The temperature is measured by a set of constantan thermocouples placed throughout the depth of the tank. The head of each thermocouple is approximately 1mm. The first one is at 2mm above the copper plate and the others are at regular intervals of 5mm above the first one. Digital Abbe refractometer with temperature compensation was used to measure the salt concentration. Measurements of the two homogeneous layers salinity were done by subtraction of a little quantity at regular intervals.

## 2.2 Experimental Procedure

The experimental tank was filled by successively introducing a solution of sodium chloride of 5 %wt concentration in water and then distilled water. The resulting stratification is 20-mm distilled water above a 20-mm salt-water layer, with the two layers separated by an interfacial layer (i.e. a gradient layer with 5 %wt/cm) of 10-mm thickness (values measured by shadowgraph system with accuracy of  $\pm 1$ mm). The free surface is at ambient temperature of 21°C, while the system is heated from below with the bottom copper plate held at a constant temperature of 60°C.

The visualizations of the flow patterns were made by a classical 2D-PIV system. Two CCD cameras (see Fig. 1) were simultaneously used, one to visualize the overall flows throughout the stratified layers in a frame approximately equal to the half the tank's length because the flow is symmetric at the overall length of the experimental tank (see Fig. 2). The second camera was used to visualize a fixed frame of 15mm $\times$ 12mm (see Fig. 2) aimed at the thickness of the interfacial layer. This latest camera is used to depict out more details of convective flows across and nearby the interfacial layer. The photography of particles images was provided by illumination in the form of a plane with a thin vertical sheet of light produced by passing a 20mW He-Ne laser beam through a cylindrical lens. The liquids of the stratification were seeded with standard PIV plastic spherical particles.

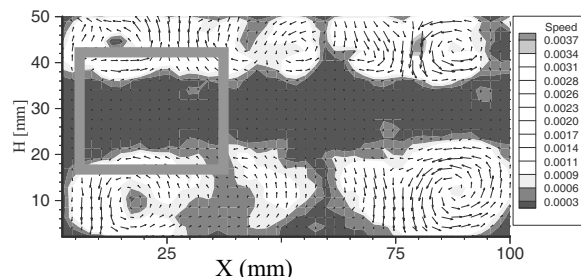
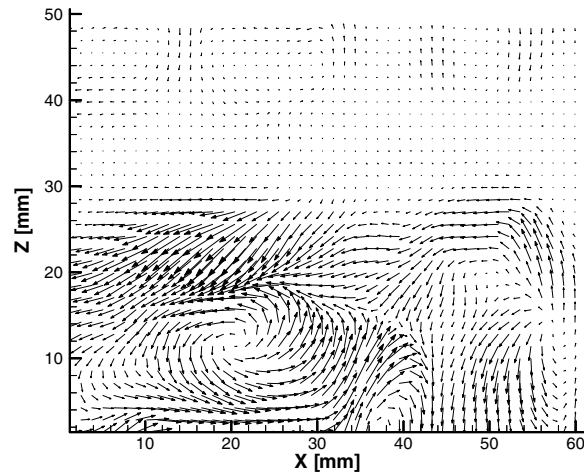


Figure 2: The frame indicates the zoom in position in interface

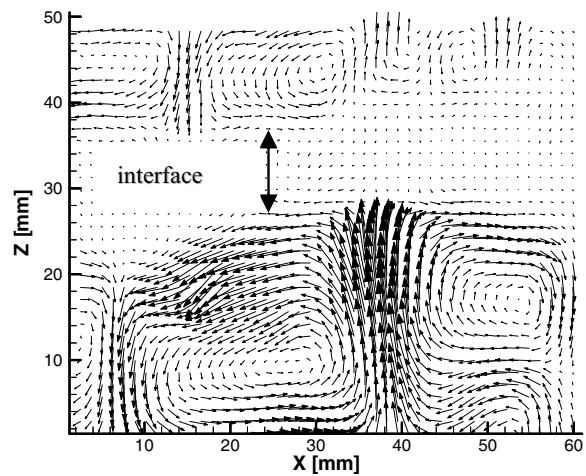
## 3 Results and discussion

The flow visualizations in the right half of the experimental tank presented in Fig. 3 reveals that convective flows initiated in the lower layer (Fig. 3.a), and subsequently in the upper layer (Fig. 3.b) and no convection intrude into the interfacial layer. For more details, vertical velocity profile is plotted in Fig. 4; it reveals, also, that velocity across the interfacial layer is insignificant. Thus, the convection is restricted to the upper and lower layer, only. The same observations were depicted by other techniques as was cited by [Abdeljabar and Safi (2001)]. In such a case the potential energy of a salt gradient layer is greater than instable heating energy.

The visualizations (Fig. 3.b) reveal that convective flows have vortices patterns in the upper and lower layer. Both in the upper and in the lower layer, vortices are in contra-rotation, however, the adjacent (i.e. face-to-face) vortices in the upper and lower layer are in co-rotation. Therefore, the convective vortices in the upper and lower layer induce sheared flow across the interface. Figure 5 illustrates the convective flows, which occur through the stratification. It is quite clear, that interfacial layer is sheared periodically owing to these convective flows patterns in the upper and lower homogeneous layers. Similarly, each two adjacent vortices in upper and lower layers induce a local shear flow at the edges of the interfacial layer. They are in opposite directions at the upper and lower edges of the interfacial layer at any given location (Fig. 3). The flow reversal induces a shearing of the interfacial layer. This implies that the interface is sheared in a periodic pattern along its edges. The length of each sheared zone is equal to the horizontal length of vortex that is laying on the interfacial layer edge (i.e. the half length of the propagating wave located at the edges of the interfacial layer). It may be asserted, however, that the way and the rate of instability for each local shear flow across the interfacial layer are similar. Given that, they have the same scales. It is noticeable that we restricted the subsequent study to a local shear flow across the interfacial layer. Hence, the evolution of the instability of a local sheared flow across the in-



(a)  $t=2$  min



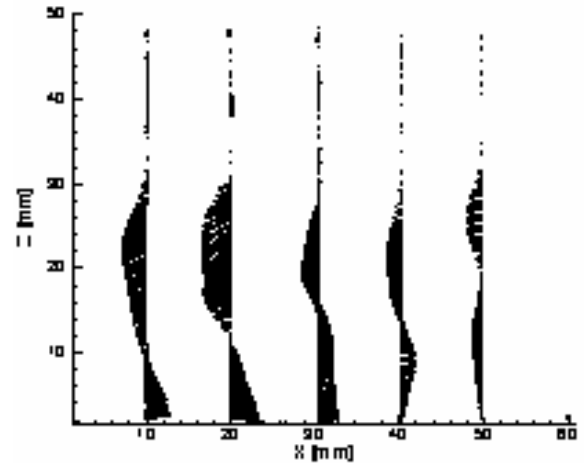
(b)  $t=5$  min

Figure 3: The evolution of the velocity fields of the stratification

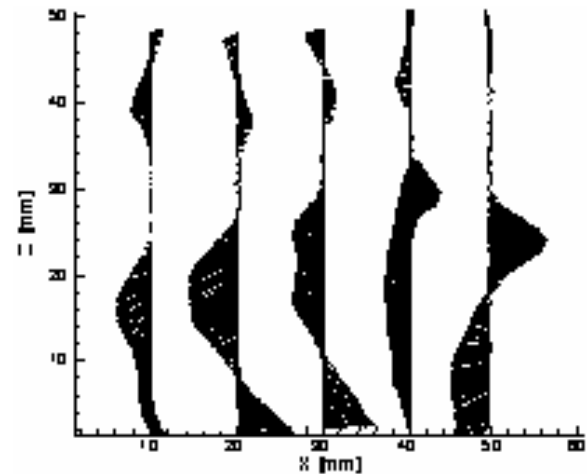
terfacial layer was depicted by the second camera aimed at the interface.

There is second phenomenon acting on stability of the interfacial layer, which cannot be ignored, namely that double-diffusion. One has to emphasize the fact that double-diffusion involves of the evolution of stability. Given that it is observed that both phenomena lead to numerous mechanisms of instability of the interfacial layer.

Basically, the instability is focused on the kind and the rate of the local shear convective flows within the interfacial layer. All convective flows that occur through the interfacial layer during the experimental study are illustrated in Fig. 6. Three



(a)  $t=2$  min



(b)  $t=5$  min

Figure 4: Vertical velocity profiles through the stratification at different location

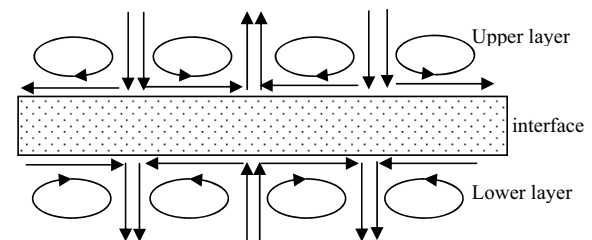


Figure 5: Synoptic of the flow at the edges of the interfacial layer

cases of flow are identified. In the following sections, the description of each case is explained.

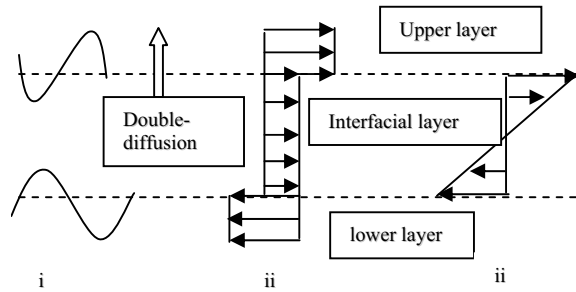


Figure 6: Sketch of the steps of the interface instability: i) Double-diffusion; ii) Kelvin Helmholtz instability and iii) Kelvin Helmholtz instability

### 3.1 Case 1 (Fig. 6-i): zero-flow through the interfacial layer

Figures 7.a-e show the field of the velocity of convective flows through the interfacial layer and its edges and the vertical velocity profile across the interfacial layer. It is clear that the interfacial layer stagnant for a time of 24min (Fig. 7.a). Thus, the shear flow at the edges of the interface can't generate any internal flow across the interfacial layer. The disturbances (i.e. perturbation) within the interfacial layer is due to the propagating waves of convective flows at the edges of interfacial layer are damped; each disturbance is subject to a counter-acting force of gravity (i.e. the potential energy of the stable salt gradient layer or the interfacial layer).

While the interfacial layer is sheared by convective flows at its edges, double-diffusion decreases the stability of the interfacial layer. The diffusion of salt across the interfacial layer makes the potential energy of the salt gradient layer (i.e. interfacial layer) weaker. The salinity of the upper layer increases, however, in the lower layer decreases. Even, the temperature at the lower layer is large than those of the upper layer due two the molecular diffusion of heat across the salty gradient layer. Then the buoyancy effect is more significant through the gradient layer. Simultaneously with shearing convective flows, presumably the edges of the interfacial layer should be smoothly eroded, but at this stage the kinetic energy is unable to make erosion of the potential energy of interfacial layer. Therefore, we come to the conclu-

sion that instability of the interfacial layer is enhanced by the effect of the double-diffusion phenomenon, only. It is worthwhile to notify that the intensity of the sheared flow is varying too, due to the variation of the temperature and salt concentration in the upper and lower layer. These variations will carry to an extreme after which the kinetic energy of the convective flows can trigger off the erosion of the interfacial layer. In such complex process, for a time 24-min, the double-diffusion across the interfacial layer enhances notably the effect of sheared flows, which is why the instability of the interfacial layer occurs dominant in other form.

### 3.2 Case 2 (Fig. 6-ii): relative flow within the interfacial layer

Subsequently at time  $t = 24\text{min}$  to  $t = 71\text{min}$ , the horizontal flow at the upper edge of the interfacial layer causes the liquid of the interfacial layer (which are initially at rest) to begin moving from its upper edge into the interior of the layer (Fig. 6.b-c). The main causes responsible for moving the interfacial layer liquids are shear stress, not buoyancy (i.e. convection). Further, Figs (7.b and c) show a slight jump in the profile of the velocity at the boundary of the upper homogeneous layers and the middle gradient layer. It has been reported that this kind of flow can induce an instability of the Kelvin-Helmholtz type [e.g. Chandrasekhar (1961)]; when the wave number,  $K$ , is in the direction of velocity vector and satisfy the following condition:

$$K > k_{\min} = \frac{g(\rho_{\text{int}}^2 - \rho_{\text{sup}}^2)}{\rho_{\text{int}} \rho_{\text{sup}} (U_{\text{sup}} - U_{\text{int}})^2}.$$

Usually, a patch of vortices comes with this form of instability; hence, in our experimental study only a relative flow is observed. During the relative flow that acts on the stratification, no mixing zone or overturning behaviour is observed at the upper edge of the interfacial layer (Fig.7. b-c). Besides, a worthwhile observation is made between the interfacial layer and the lower saltier layer; a relative flow establishes across the interfacial layer and the saltier lower layer. Figures 7.b-d, the profile of velocity shows a flow in opposite directions; and a zero flow is observed at the interface between saltier lower layer and the interfacial layer.

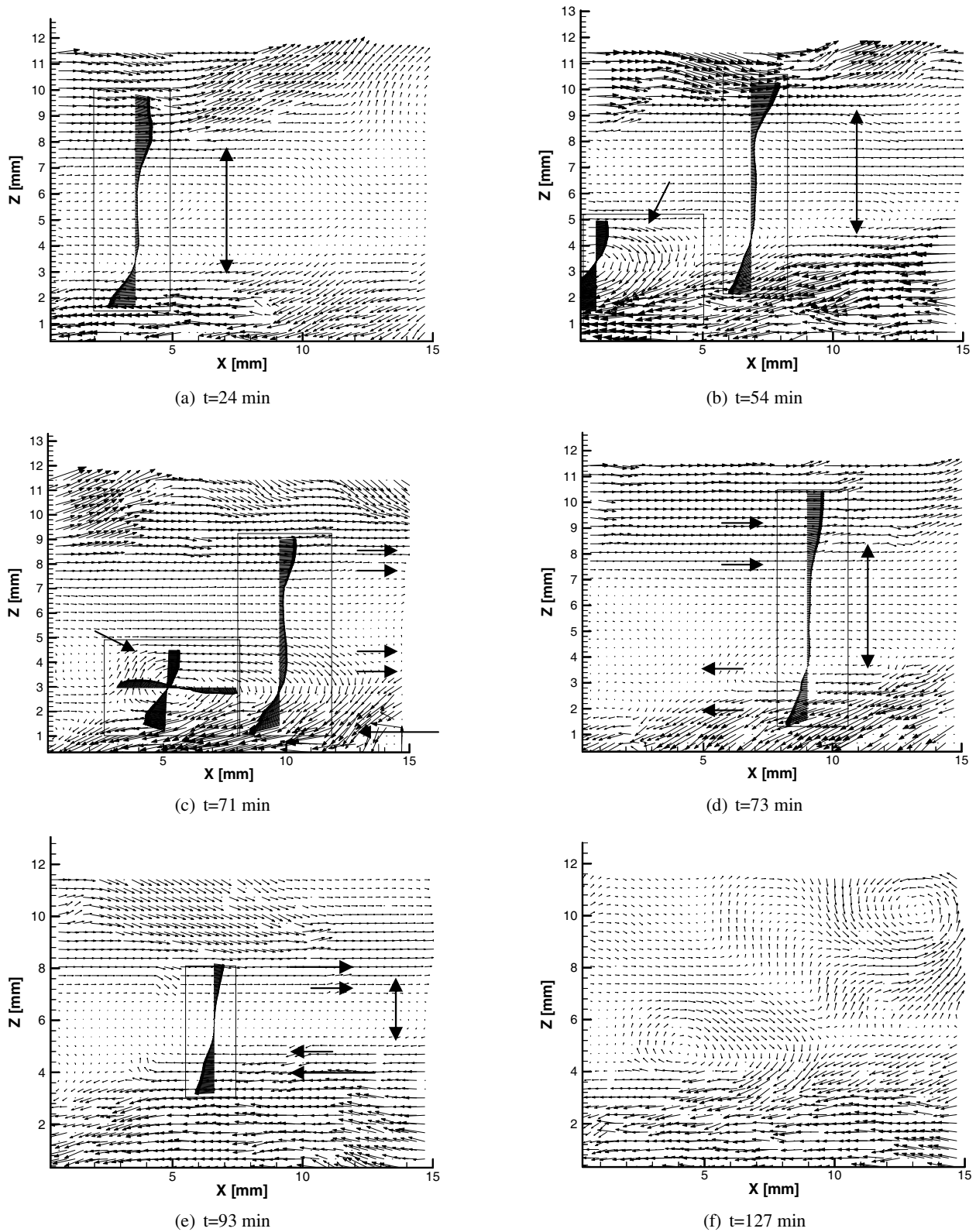


Figure 7: Visualization by PIV of the velocity fields through the interface and its edges (local observation) The horizontal arrows show the flow direction at the edges of the interfacial layer. The vertical one the thickness of the interfacial layer The frame showed a vertical profile of velocity through the interface or an overturning when it is pointed out by an oblique arrow

This kind of flow leads to an instability type, Kelvin-Helmholtz [e.g. Chandrasekhar (1961)], and occurs when Rayleigh's and Fjortoft's criterion are fulfilled [e.g. Baines and Mistudera (1994)]. Thus, visualisations allow us to conclude that a second form of Kelvin-Helmholtz instability originates at the lower edge of the interfacial layer also producing a patch of vortices. Figures 7-b and 7-c show overturning flow behaviour (i.e. a local circulating region with closed streamlines) at the lower edge of the interfacial layer. The vortices in the lower homogeneous layer due to convection are in counter-rotation, while the vortex in the lower layer and the overturning flows are in co-rotation. This implies that the overturning flows are induced by the viscosity effects associated with the convective flows. Thus, the overturning flows occur due to the horizontal propagating waves of the convective flows. It was found that a criterion for the stability is expressed in terms of the Richardson number. The necessary condition for stability is that the Richardson number is everywhere greater than ( $R_i > 1/4$ ). For our experiment, the Richardson number at time  $t=71$ min was computed from experimental data (see Figs. 7-c, 9, 10). For such instability, the experimental Richardson number is considered to have the following form  $R_i = \frac{g \cdot \Delta \rho \cdot \delta}{\rho_m \Delta u^2}$  (where  $g$ : the gravitational acceleration,  $\Delta \rho$ : the density difference across the adjacent plan,  $\delta$ : the thickness of the adjacent plan,  $\rho_m$ : the average density across the adjacent plan and  $\Delta u$  is the horizontal velocity component difference at the adjacent plan). At time  $t=71$ min, the experimental results give a value of Richardson number equal to  $R_i=0.0053$ . This result and the experimental observations demonstrate that the instability occurred is of the Kelvin-Helmholtz type. This form of instability acts mechanically on the stable interfacial layer liquids. While the potential energy of the interfacial layer becomes weaker due to double-diffusion, the kinetic energy of the convective flows of the lower layer combined with the effect of double diffusion to progressively erode the interfacial layer. The horizontal shear flow erodes the lower edge of the interfacial layer by sweeping and tearing off small fluid element. These elements are stirred by the overturning (so-

called eddy) and transported by shear flow between two vortices. This phenomenon is depicted in Figs 7-b and 7-c. As a result, we observe the increase of the lower layer and the decrease of the interfacial layer.

### 3.3 Case 3 (Fig. 6-iii): sheared flow across the interfacial layer

At time  $t=91$ min, a sheared flows appears across the interfacial layer as it is showed in Figure (6-e). The boundary conditions of such flows can be described by continuous variation of both density and velocity. This is due to the dynamics of the stratification, similar to the theory for the same flow and conditions [e.g. Chandrasekhar (1961)]. It occurs when the Richardson number is less than  $1/4$ . The experimental Richardson number is calculated from  $R_i = \frac{g \cdot \Delta \rho \cdot d}{\rho_m \Delta u^2}$  (where  $\Delta \rho$ : the density difference across the interfacial layer,  $d$ : the thickness of the interface,  $\rho_m$ : the overage density across the interface and  $\Delta u$  is the horizontal velocity component difference at the edge of the interface). At time  $t=93$ min, the experimental results (Fig.10, 11 and 7.e) give a value of Richardson number equal to  $R_i=0.0186$ . This result and the experimental observations again demonstrate that the instability is of the Kelvin-Helmholtz type. The signature of this kind of instability is recognized by the patterns of the flow across the interface. Figure (8) shows the evolution of the flow patterns into the interfacial layer. The vortices extending into the interfacial layer in between two opposing vortices in the upper and the lower layer are in counter rotation, while, the opposing vortices are in co-rotation. In such a case, the mechanism of instability is essentially kinematical. It is described as follows. The motion of the vortices at the interfaces is a pair of waves propagating in the opposite directions, each being affected by the velocity field of the other. The velocity fields of the interfacial vortices are the sum of the velocity fields of each interfacial wave as if they acted in isolation. Therefore, the interfacial flow between two vortices accelerates due to the sum of the two components of velocity for each two vortices. Thus, the vortices extending into the interfacial layer are stretched and squeezed. Fig-

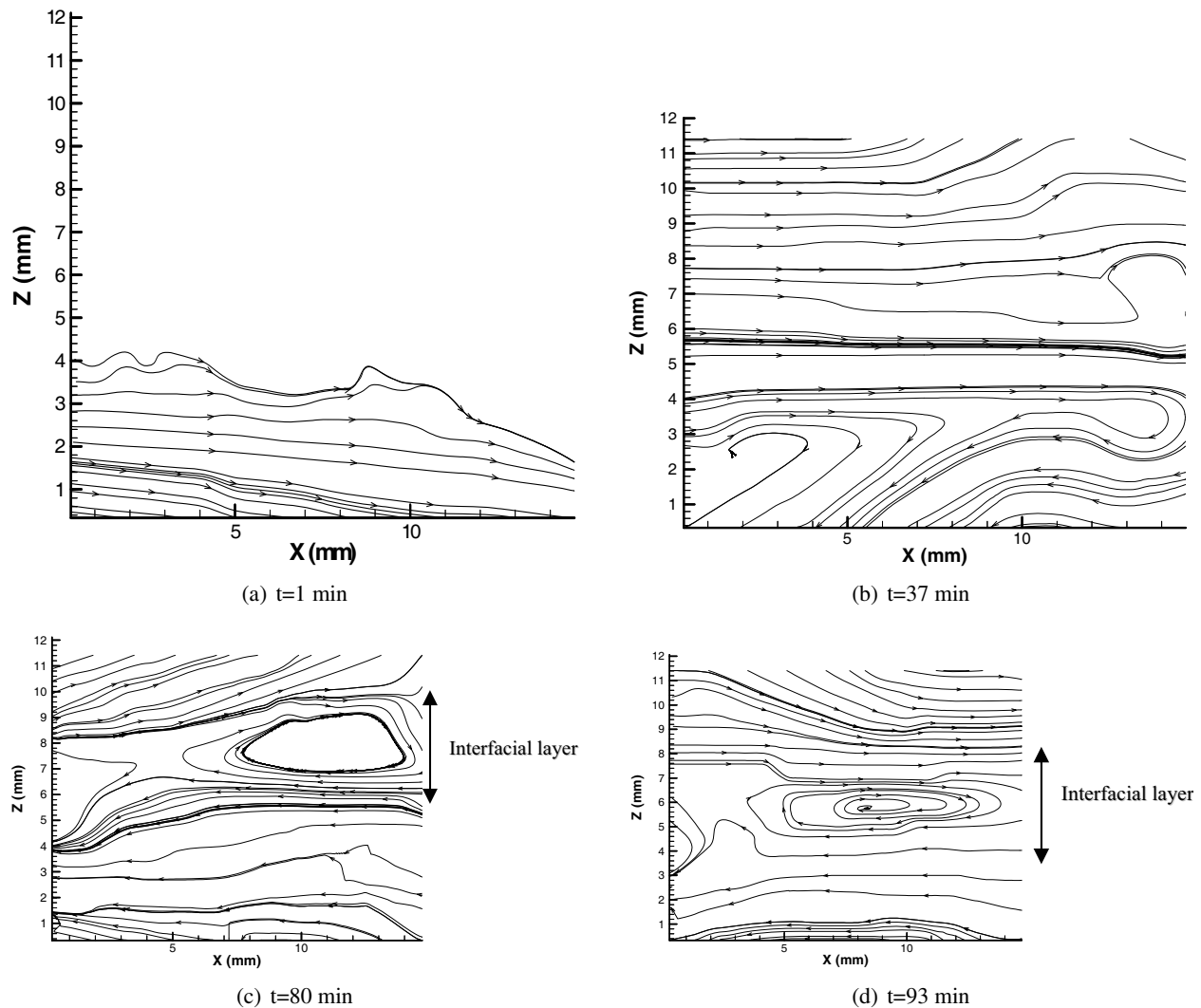


Figure 8: The streamlines of the flow within the interface and its edges (local observation). A close stream lines (eddy) appears in the interface thickness as it is shown in c) and d)

ures (8.c and 8.d), we can observe the effect of the both phenomena; the vortices extending into the interfacial layer have an elliptical shape, and are subsequently torn the interfacial layer. The observations (Fig. 7-e and 8-c-d) show a patch of vortices that mixed fluid at the interfacial layer. These vortices grow in time until the interfacial layer splits and decays. This phenomenon was observed by shadowgraph system [Abdeljabar and Safi (2001)]. This form of Kelvin-Helmholtz instability occurs when the destabilizing effect of the shear flow within the interface region is large and the potential energy of the gradient layer (i.e. the interfacial layer) is too weak to overcome

the destabilizing effect of the buoyancy gradient. However, the first two forms of instability of the Kelvin-Helmholtz type act on the interfacial layer leading to the third form of Kelvin-Helmholtz instability to occur.

#### 4 Summary

The present experimental study leads to conclude that in addition to the phenomenon of double-diffusion, the instability of the interfacial layer is due to numerous variants of the Kelvin-Helmholtz instabilities (Fig.8). The first occurs when the convective flows in the upper layer cause the liquid of the interfacial layer to flow.



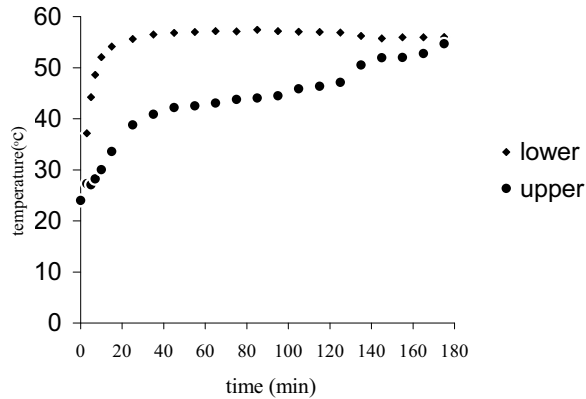


Figure 9: Evolution of bulk temperature in homogeneous layers

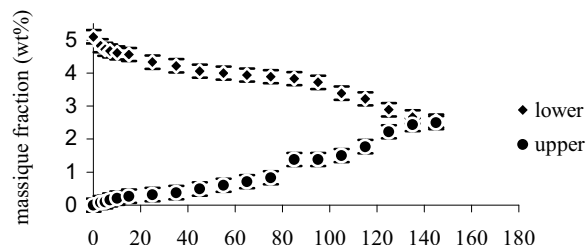


Figure 10: Evolution of bulk concentration of the layers

The second occurs when the adjacent surface between the interfacial layer and the upper edge of the lower layer is sheared. These two mechanisms act, in addition to the effect of the double-diffusion across the interfacial layer, to erode the interface shape (making it thinner).

The third form of Kelvin-Helmholtz instability occurs when a velocity gradient appears across the interfacial layer. The shear flow within the interfacial layer induces destructive shearing of the interfacial layer. This mechanism leads to considerable homogenisation of the entire stratification.

**Acknowledgement:** This work has been done in the context of a project of cooperation between DGRST Tunisia and CNRS France.

## References

**Abdeljabar, R.; Safi, M.J.** (2000): Processus d'instabilité dans un milieu salin stratifié. *Entropie J.*, no. 227, pp. 62-67.

**Abdeljabar, R.; Safi, M.J.** (2001): Shear flow induced instability. *Experiments in Fluids.*, no. 31, pp. 13-18.

**Abdeljabar, R.; Onofri, F.** (2004): Observation par PIV des mécanismes d'instabilités convectives d'une zone inter faciale des deux couches miscibles stratifiées, 9<sup>ème</sup> congrès Francophonie de vélocimétrie laser, 14-17 septembre, Bruxelles, Belgique.

**Baines, P.G.; Gill, A.E.** (1963): On thermohaline convection with linear gradients. *J. Fluid. Mech.*, vol. 37, no. 2, pp. 289-306.

**Baines, P.G.; Mitsudera, H.** (1994): On the mechanism of shear flow instabilities. *J. Fluid. Mech.*, vol. 276, pp. 327-342.

**Balmforth, N.J.; Lewellyn Smith, S.G.; Young, W.R.** (1998): Dynamics of interfaces and layers in a stratified turbulent fluid. *J. Fluid. Mech.*, vol. 355, pp. 329-358.

**Barenblatt, G.I.; Bertsch, M.; Dal Passo, R.; Prostokishin, V.M.; Ughi, M.** (1993): A mathematical model of turbulent heat and mass transfer in stably stratified shear flow. *J. Fluid, Mech.*, vol. 253, pp. 341-358.

**Bars, M.; Davaille, A.** (2002): Stability of thermal convection in two superimposed miscible viscous fluids. *J. Fluid. Mech.*, vol. 471, pp. 330-363.

**Bergman, T.L.; Incorpora, F.P.; Viskanta, R.** (1987): Interaction of external and double-diffusion convection linearly salt-stratification systems. *Experiments in fluids.*, no. 5, pp. 49-58.

**Chandrasekhar, S.** (1961): *Hydrodynamic and hydromagnetic stability*. Clarendon Press, Oxford.

**Drazin, P.G., Reid, W.H.** (1981): *Hydrodynamic instability*. Cambridge university Press.

**Drazin, P.G.** (1989): *Internal gravity waves and shears instability*. In waves and stability in continuous Media. ed.A.Donato & S.Giambo Edit1.

**Galmiche, M.; Hunt, J.C.R.** (2002): The formation of shear and density layers in stably stratified turbulent flows: linear processes. *J. Fluid. Mech.*, vol. 455, pp. 243-262.

**Harindra, J.S.F.; Robert, R. L.** (1985): On the

nature of the entrainment interface of a two-layer fluid subject to zero-mean-shear turbulence. *J. Fluid. Mech.*, vol. 151, pp. 21-53.

**Harindra, J.S.F.** (1987): The formation of a layered structure when a stable salinity gradient is heated from below. *J. Fluid. Mech.*, vol. 182, pp. 525-541.

**Hull, J.R.; Mehta, J.M.** (1987): Physical model of gradient zone erosion in thermohaline systems. *J. heat Mass Transfer.*, vol. 30, no. 6, pp. 1027-1036.

**Huppert, H.E.** (1971): On heating stable salinity gradients from below. *J. Fluid. Mech.*, vol. 78, pp. 821-854.

**Khantha, L.H.; Phillips, O.M.; Azad, R.S.** (1977): On turbulent entrainment at a stable density interface. *J. Fluid. Mech.*, vol. 79, pp. 753-768.

**Linden, P.F.** (1975): The deepening of a mixed layer in a stratified fluid. *J. Fluid. Mech.*, vol. 71, pp. 385-405.

**Linden, P.F.; Shirtcliffe, T.G.L.** (1978): The diffusive interface in double-diffusive convection. *J. Fluid. Mech.*, vol. 87, no. 3, pp. 471-432.

**Park, Y.-G.; White, J.A.; Gnanadeskian, A.** (1994): Turbulent mixing in stratified fluids: layer formation and energetic. *J. Fluid. Mech.*, vol. 279, pp. 279-311.

**Poplowsky, C.J.; Incorporera, F.P.; Viskanta, R.** (1981): Mixed layer development in a double-diffusion, thermohaline system. *Journal of Solar Energy engineering*, 103, pp. 351-359.

**Sulliva, G. D.; John; List. E.** (1994): On mixing and transport at a sheared density interface. *J. Fluid. Mech.*, vol. 273, pp. 213-239.

**Turner, J.S.** (1968): The behavior of a stable salinity gradient heated from below. *J. Fluid. Mech.*, vol. 33, no. 1, pp.183-200.

**Turner, J.S.** (1973): *Buoyancy effects in fluids.* Cambridge at the university press.

**Turner, J.S.** (1991): Convection and mixing in the oceans and earth. *Phys. Fluids.*, A3 (5), pp. 1281-1232 .

**Veronis, G.** (1968): Effect of a stabilizing gradient of solute on thermal convection. *J. Fluid.*

*Mech.*, vol. 34, pp. 315-336.

**Walton, I.C.** (1982): Double-diffusive convection with large variable gradients. *J. Fluid. Mech.*, vol. 125, pp.123-135.

**Wright, J.H.; Loehr, R.I.** (1976): The onset of Thermohaline convection in linearly-stratified horizontal layer. *Journal of Heat Transfert.*, pp. 558-563.

**Wyatt, L.R.** (1978): The entrainment interface in a stratified fluid. *J. Fluid. Mech.*, vol. 86, pp. 293-311.

**Zangrando, F.; Bertran, L.A.** (1985): The effect of variable stratification in linear double-diffusive stability. *J. Fluid. Mech.*, vol. 151, pp. 55-79.